

Supplemental Material for

**Magnetic-Field-Induced Ferroelectric states in Centrosymmetric
 $R_2\text{BaCuO}_5$ ($R = \text{Dy}$ and Ho)**

Premakumar Yanda¹, F. Orlandi², P. Manuel², N. Boudjada³, J. Rodriguez-Carvajal⁴, and
A. Sundaresan^{1*}

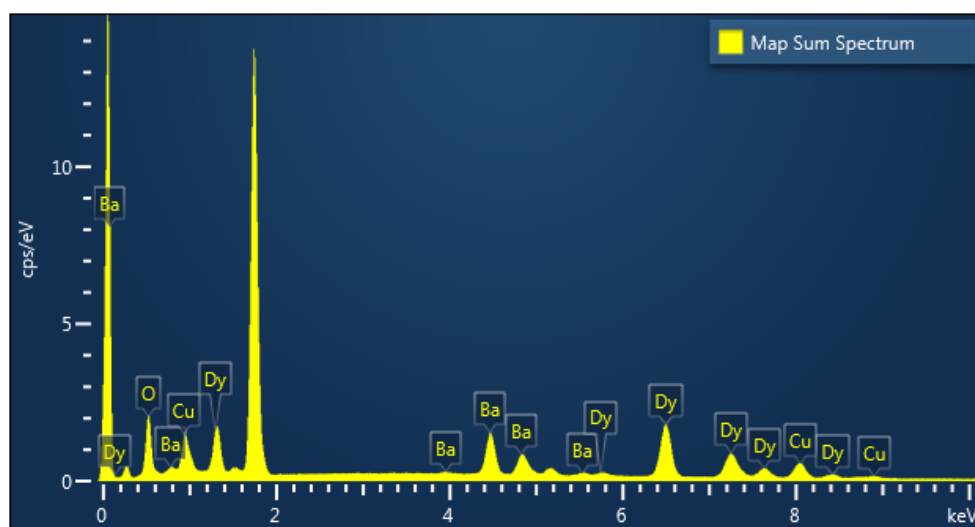
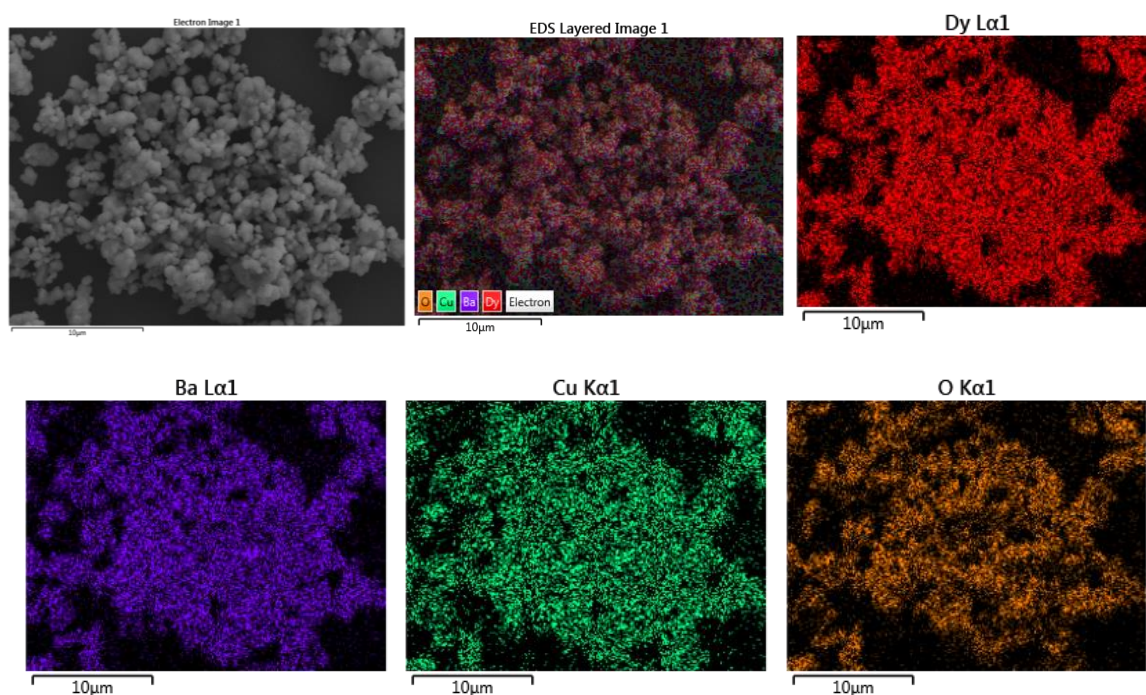
¹*School of Advanced Materials, and Chemistry and Physics of Materials Unit, Jawaharlal
Nehru Centre for Advanced Scientific Research, Jakkur P.O., 560064, India.*

²*ISIS Facility, Rutherford Appleton Laboratory, Harwell Campus, Didcot, OX11 0QX, UK.*

³*Université Grenoble Alpes, CNRS, Institut Néel, 38000 Grenoble, France.*

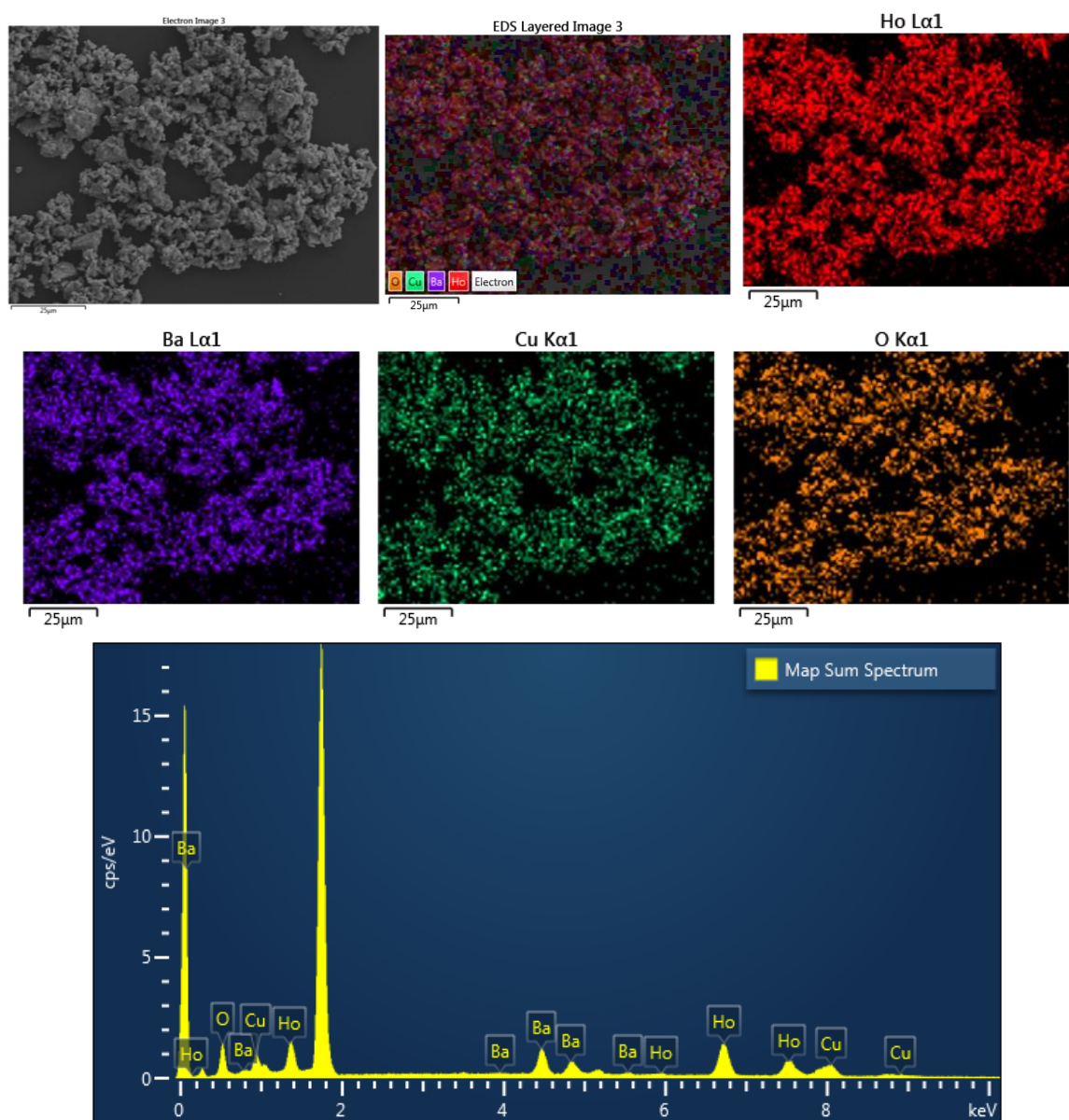
⁴*Institut Laue Langevin, Diffraction Group, CS 20156 -38042 Grenoble CEDEX 9, France.*

Figure S1. SEM images and EDS spectra for Dy₂BaCuO₅. Table shows the quantification results obtained from the EDS analysis.



Element	Line type	Apparent Concentration	K Ratio	Wt%	Wt% sigma
O	K series	2.47	0.00831	17.61	0.22
Cu	K series	1.73	0.01729	9.88	0.17
Ba	L series	3.55	0.03323	21.87	0.19
Dy	L series	7.67	0.07672	50.64	0.26
Total				100	

Figure S2. SEM images and EDS spectra for $\text{Ho}_2\text{BaCuO}_5$. Table shows the quantification results obtained from the EDS analysis.



Element	Line type	Apparent Concentration	K Ratio	Wt%	Wt% sigma
O	K series	1.70	0.00572	15.64	0.46
Cu	K series	1.45	0.01449	9.59	0.39
Ba	L series	2.85	0.02668	21.56	0.43
Ho	L series	6.62	0.06621	53.21	0.59
Total				100	

Figure S3. Room temperature powder X-ray diffraction pattern of Dy₂BaCuO₅.

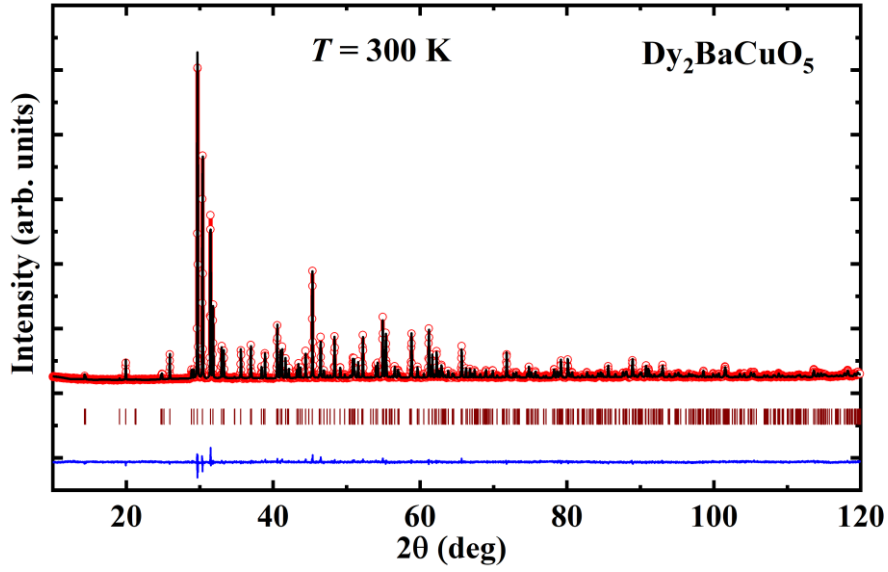


Table SI. Structural parameters of Dy₂BaCuO₅ obtained from Rietveld refinement of X-ray data collected at 300 K. Space group: *Pnma*1'; *a* = 12.2277 (1) Å, *b* = 5.6827 (1) Å, *c* = 7.1563 (1) Å, Vol: 497.264 (3) Å³; global- χ^2 = 2.12; *R*_p = 2.14, *wR*_p = 2.75.

Atom	Site	<i>x</i>	<i>y</i>	<i>z</i>	<i>B</i> _{iso} (Å ²)
Dy1	4c	0.2886 (2)	0.2500	0.1166 (4)	0.449 (58)
Dy2	4c	0.0741 (2)	0.2500	0.3962 (3)	0.620 (55)
Ba	4c	0.9051 (2)	0.2500	0.9297 (3)	0.705 (58)
Cu	4c	0.6590 (5)	0.2500	0.7125 (8)	0.384 (128)
O1	8d	0.4347 (16)	-0.0124 (29)	0.1732 (19)	1
O2	8d	0.2262 (14)	0.5079 (32)	0.3546 (26)	1
O3	4c	0.0951 (21)	0.2500	0.0731 (32)	1

Figure S4. Room temperature powder X-ray diffraction pattern of $\text{Ho}_2\text{BaCuO}_5$.

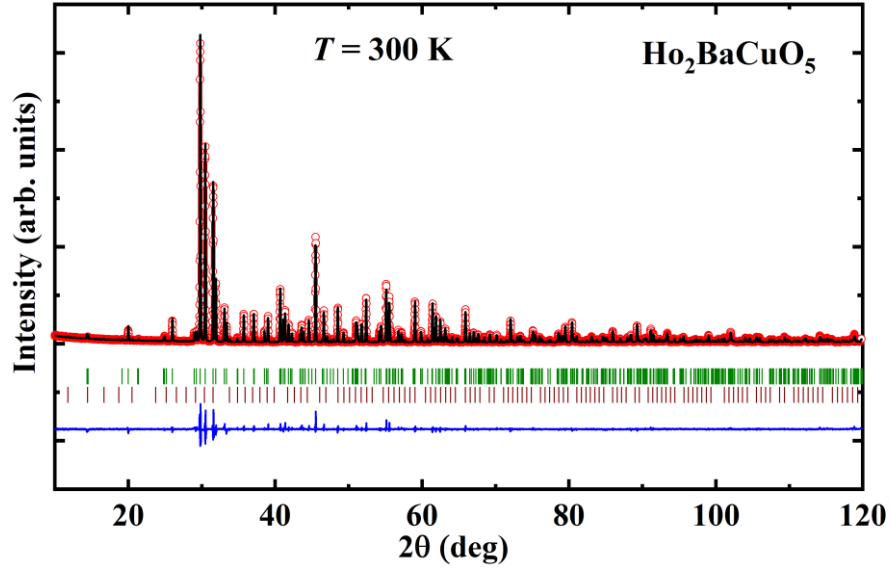


Table SII. Structural parameters of $\text{Ho}_2\text{BaCuO}_5$ obtained from Rietveld refinement of X-ray data collected at 300 K. Space group: $Pnma1'$; $a = 12.1857$ (1) Å, $b = 5.6644$ (1) Å, $c = 7.1348$ (1) Å, Vol: 492.48 (1) Å³; global- $\chi^2 = 4.05$; $R_p = 6.80$, $wR_p = 9.04$.

Atom	Site	x	y	z	B_{iso} (Å ²)
Dy1	4c	0.2883 (2)	0.2500	0.1162 (4)	1.289 (59)
Dy2	4c	0.0742 (2)	0.2500	0.3963 (3)	1.315 (57)
Ba	4c	0.9049 (1)	0.2500	0.9301 (3)	0.482 (41)
Cu	4c	0.6594 (4)	0.2500	0.7134 (7)	0.324 (103)
O1	8d	0.4333 (14)	-0.0113 (28)	0.1713 (20)	1
O2	8d	0.2268 (13)	0.5060 (30)	0.3553 (24)	1
O3	4c	0.0995 (19)	0.2500	0.0772 (31)	1

Figure S5. Refined neutron powder diffraction pattern at 25 K for $\text{Dy}_2\text{BaCuO}_5$ collected on WISH.

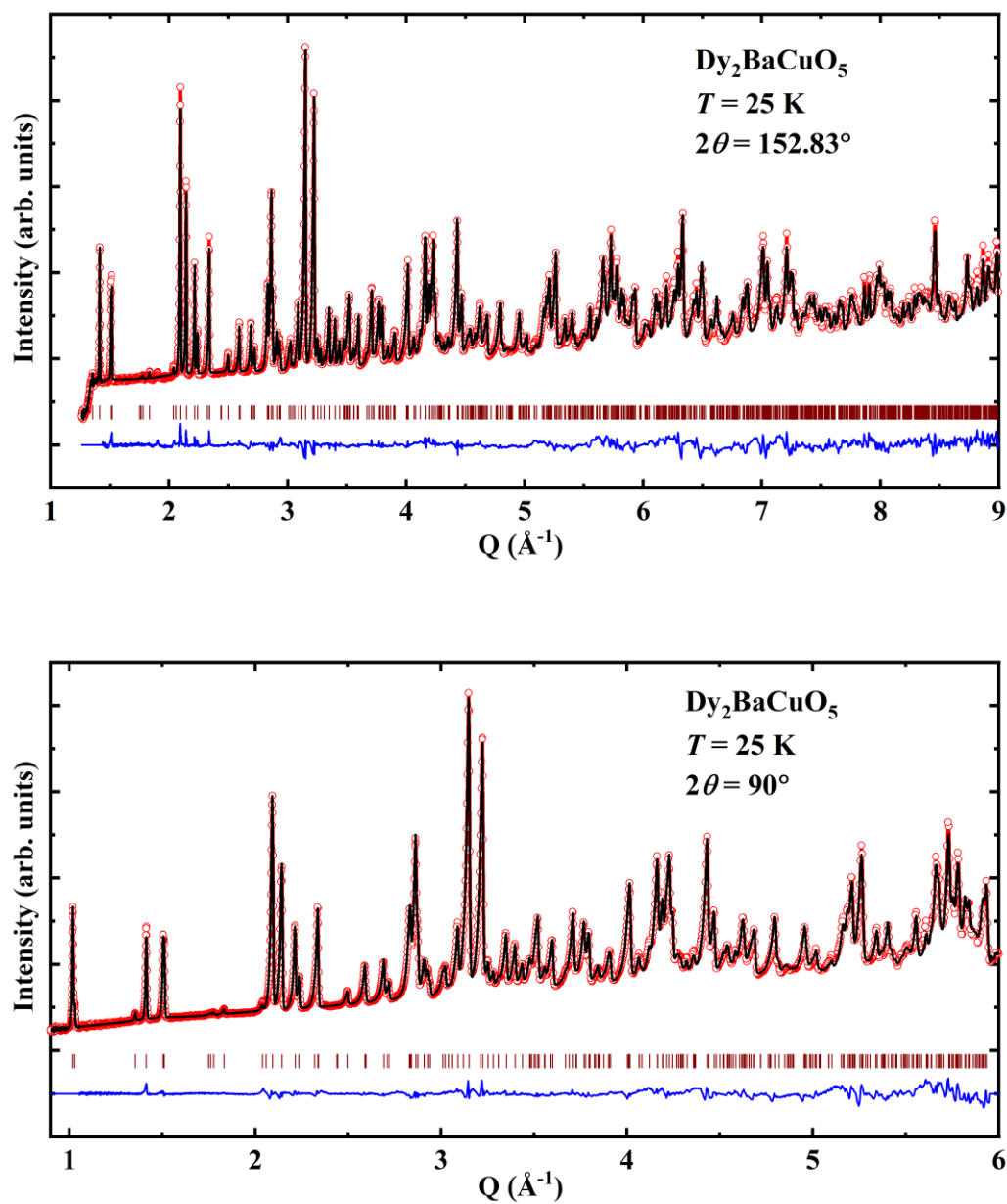


Figure S6. Refined diffraction patterns of $\text{Ho}_2\text{BaCuO}_5$ at 20 K collected on WISH. The second row of tick marks corresponds to the impurity of cubic Ho_2O_3 ($\approx 0.5\%$).

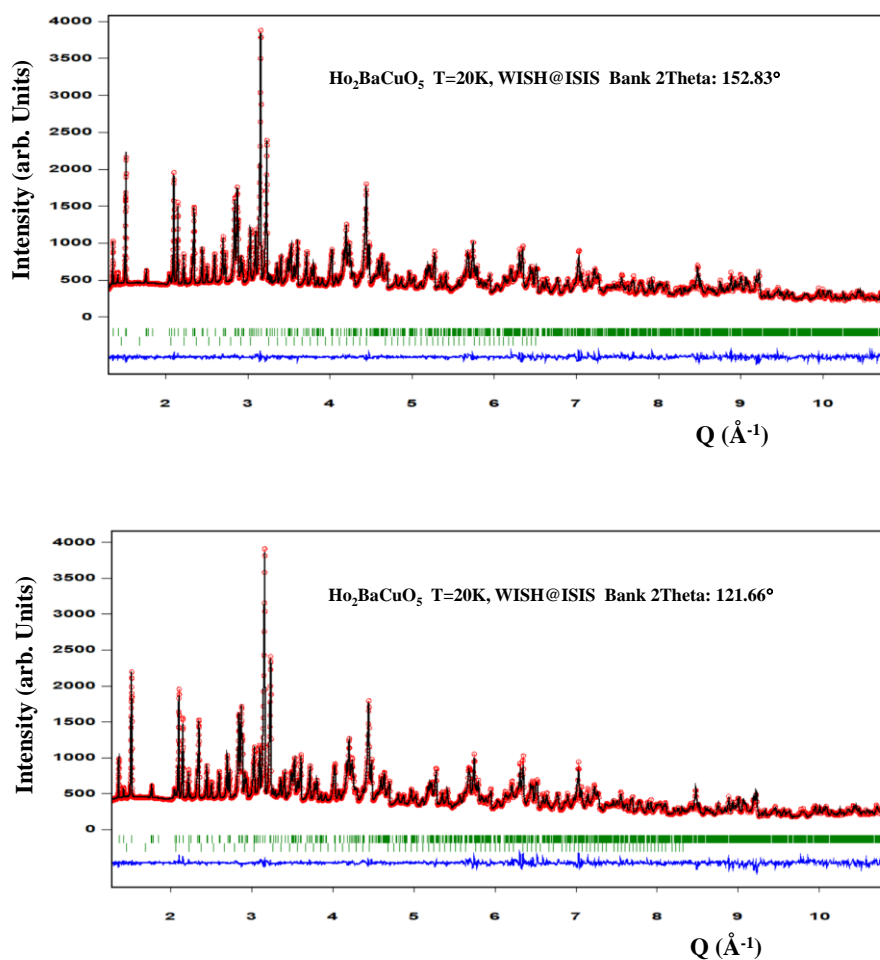


Figure S7. Left. Heat capacity of $\text{Dy}_2\text{BaCuO}_5$ measured at high temperatures under 0 T. Right. Temperature-dependent pyrocurrent data measured from 100-300 K in the absence of magnetic field after the poling.

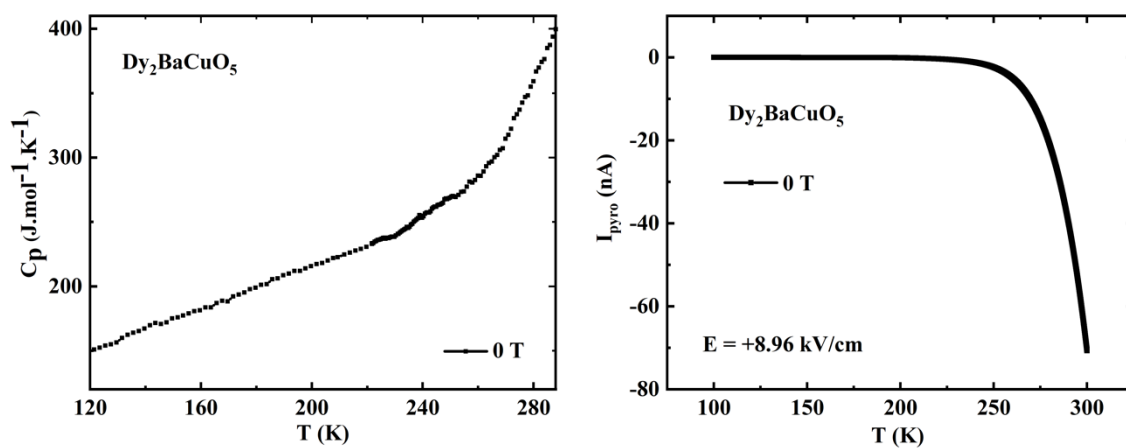


Figure S8. PE loops measured at liquid nitrogen temperature and frequency 1 Hz for $\text{Dy}_2\text{BaCuO}_5$ and $\text{Ho}_2\text{BaCuO}_5$.

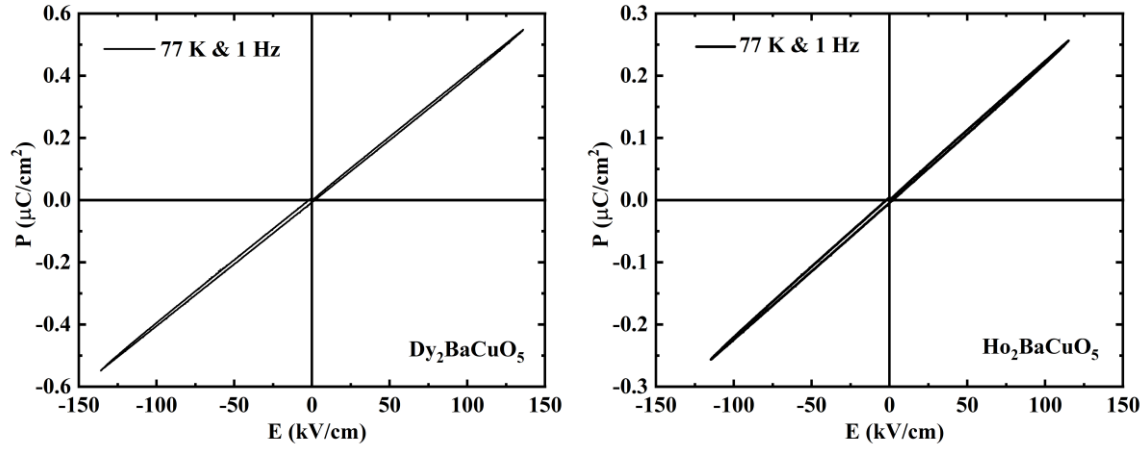


Figure S9. Inverse susceptibility for $\text{Dy}_2\text{BaCuO}_5$ (Top) and $\text{Ho}_2\text{BaCuO}_5$ (Bottom) along with Curie fit.

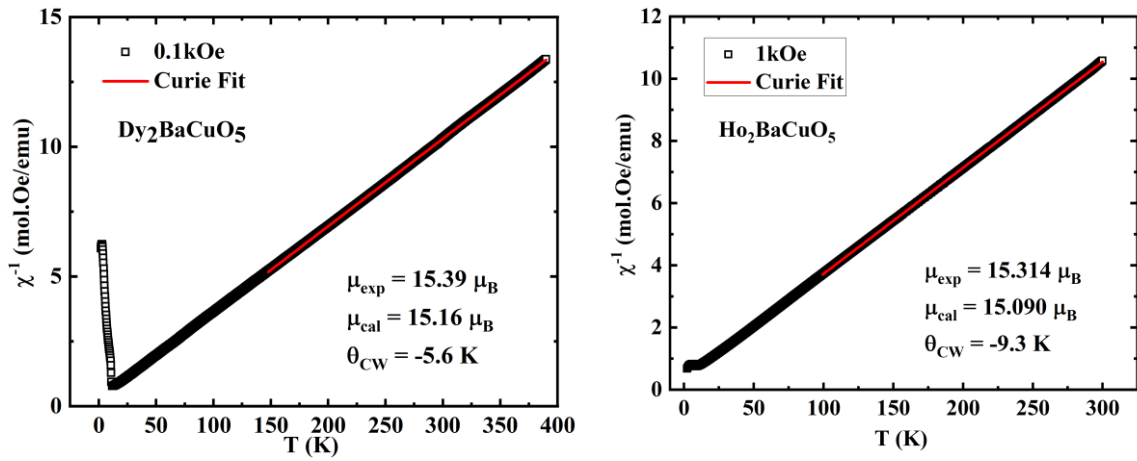


Figure S10. The derivative of magnetization with respect to the magnetic field for $\text{Dy}_2\text{BaCuO}_5$ (Top) and $\text{Ho}_2\text{BaCuO}_5$ (Bottom).

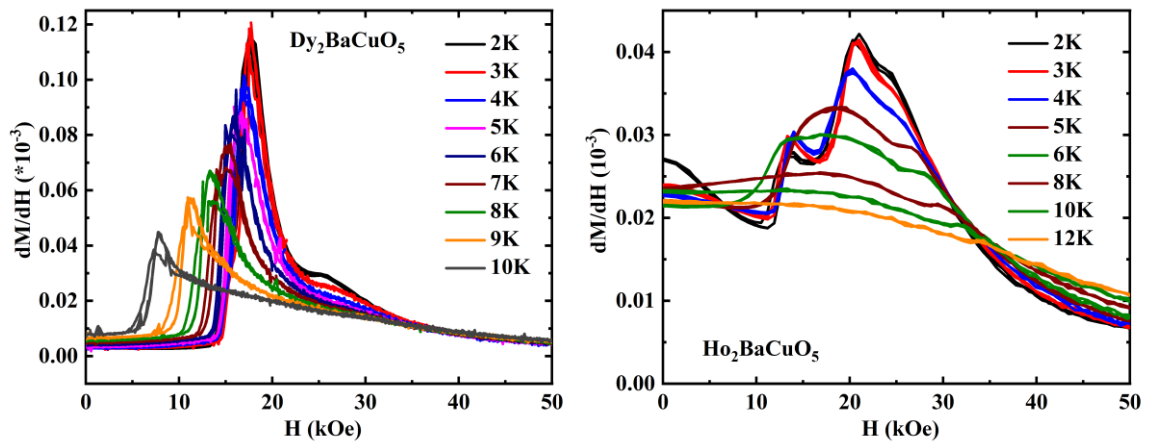


Figure S11. Magnetodielectric effect of $\text{Dy}_2\text{BaCuO}_5$. The maximum MD effect is 0.16 % which is near to rare earth magnetic ordering temperature 8 K.

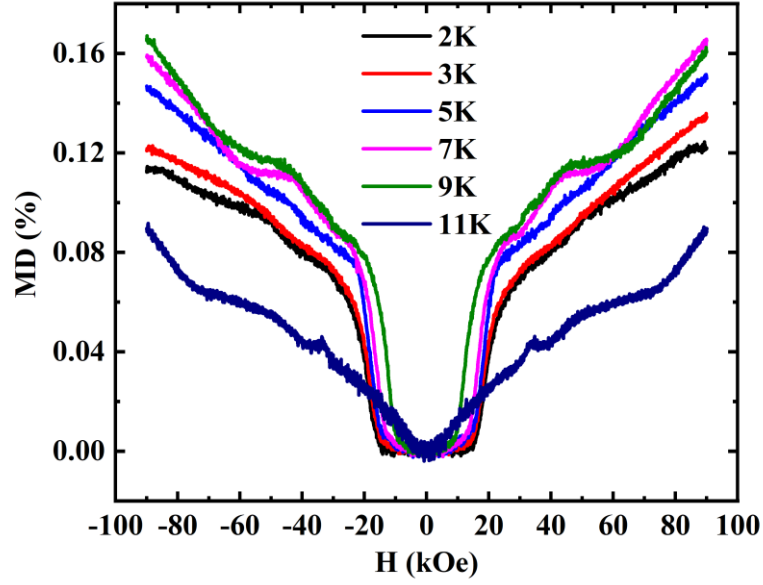


Figure S12. Electric polarization as a function of magnetic field for (a) $\text{Dy}_2\text{BaCuO}_5$ at 7 K and (b) $\text{Ho}_2\text{BaCuO}_5$ at 2 and 5 K. Solid lines represent the linear behavior of the electric polarization below metamagnetic transitions.

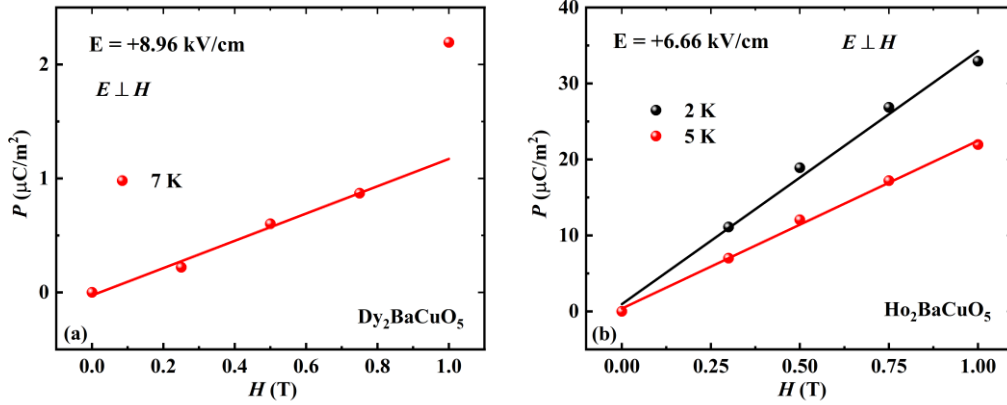


Figure S13. (a) Temperature dependent dielectric constant measured under different magnetic fields and frequency $f = 50$ kHz. (b) T -dependence of pyrocurrent recorded for different magnetic fields with the poling electric field $E = +8.96$ kV/cm. (c & d) Polarization is obtained by integrating the pyrocurrent with respect to time. The inset shows magnetic field-dependent polarization; measured in $E \parallel H$ configuration for $\text{Dy}_2\text{BaCuO}_5$.

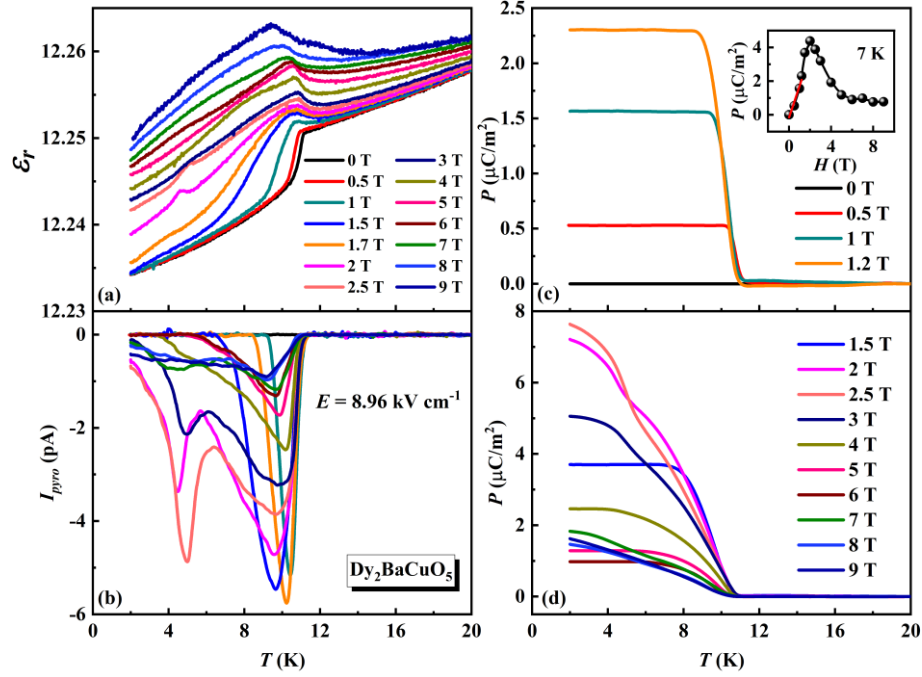


Figure S14. (a) Dielectric constant against temperature measured with frequency $f = 50$ kHz under different magnetic fields. (b) T - H dependent; measured in $E \parallel H$ configuration for $\text{Ho}_2\text{BaCuO}_5$.

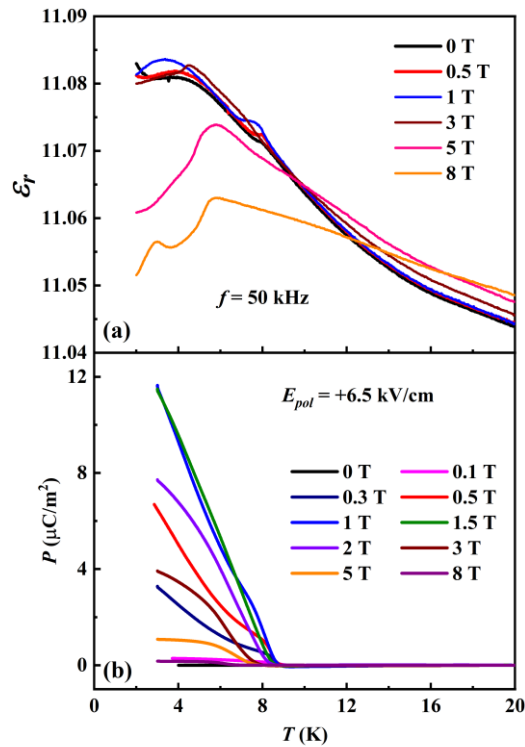


Figure S15. Refined neutron diffraction patterns at 13 K for crystal and magnetic structures of $\text{Dy}_2\text{BaCuO}_5$. We have shown the data collected on two different banks of WISH diffractometer. The refinement was carried by using the magnetic space group P_b112_1/n . The tick marks include both the nuclear and magnetic contributions.

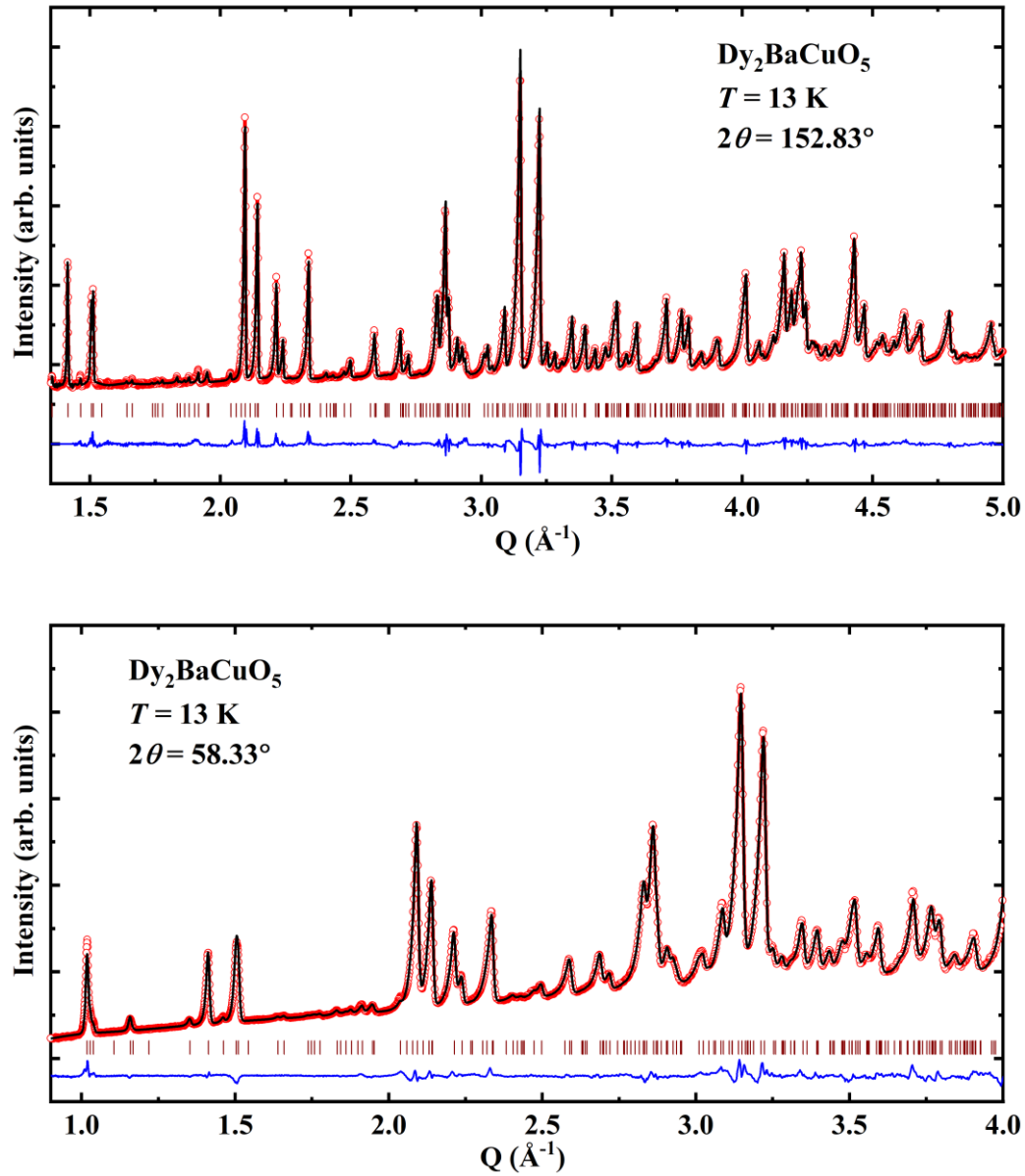


Figure S16. Refined neutron diffraction patterns at 1.5 K for crystal and magnetic structures of $\text{Dy}_2\text{BaCuO}_5$. We have shown the data collected on two different banks of WISH. The refinement was done by using the magnetic space group $Pnm'a$. The tick marks include both the nuclear and magnetic contributions.

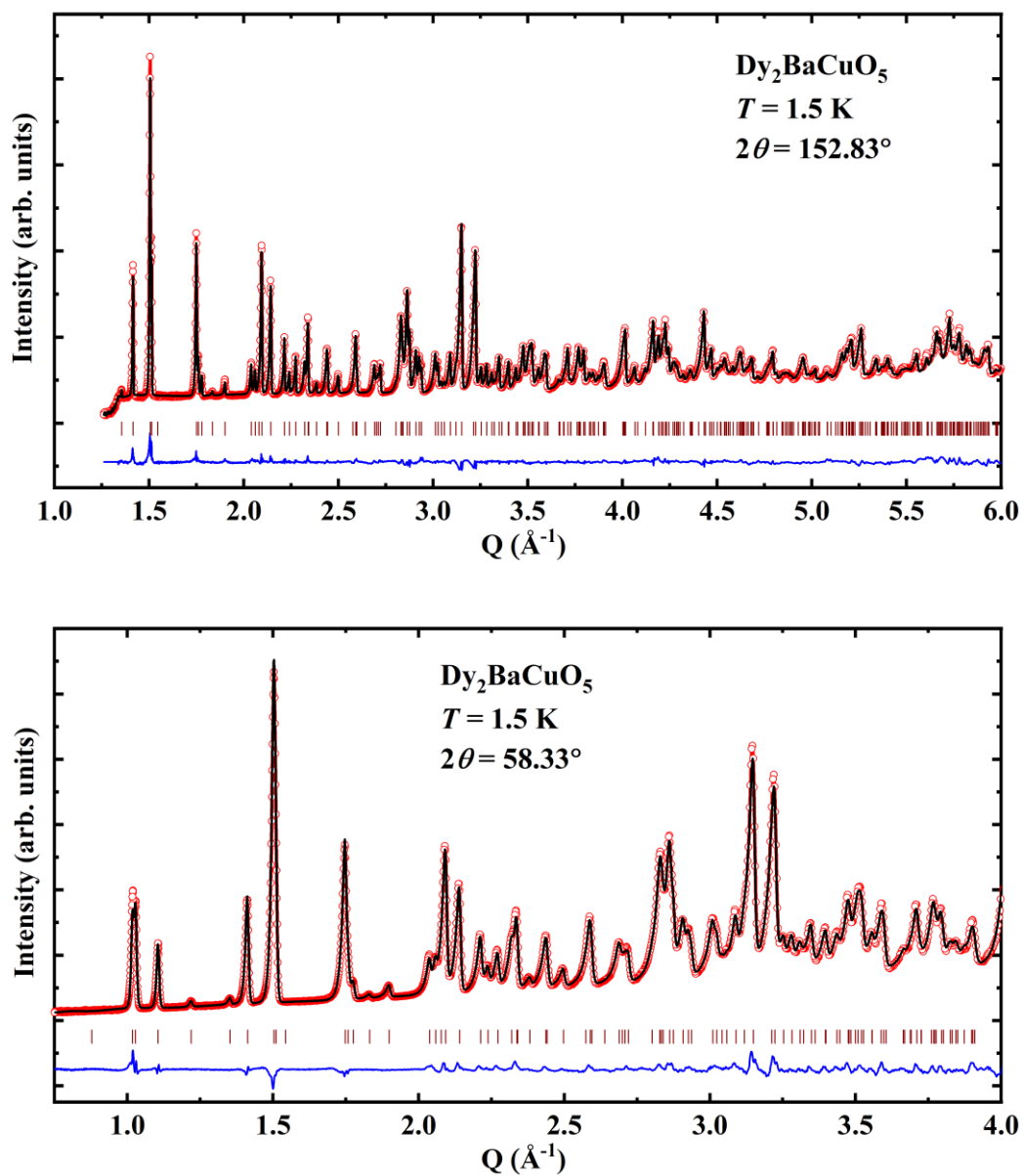


Figure S17. (Upper panel) 3D visualization of the low angle part of diffraction patterns taken on D1B ($\lambda = 2.52 \text{ \AA}$). The abrupt change of background and the simultaneous appearance of the $\mathbf{k}_{c2} = (0, 0, 0)$ magnetic peaks indicates a first-order magnetic transition. (Bottom panel) Details of the evolution of diffraction patterns of $\text{Ho}_2\text{BaCuO}_5$ around the transition at $T_N^{\text{Ho}} \approx 8 \text{ K}$. The indexing of peaks (blue for $\mathbf{k}_{c1} = (0, \frac{1}{2}, 0)$, red for $\mathbf{k}_{c2} = (0, 0, 0)$) is given with respect to the paramagnetic unit cell.

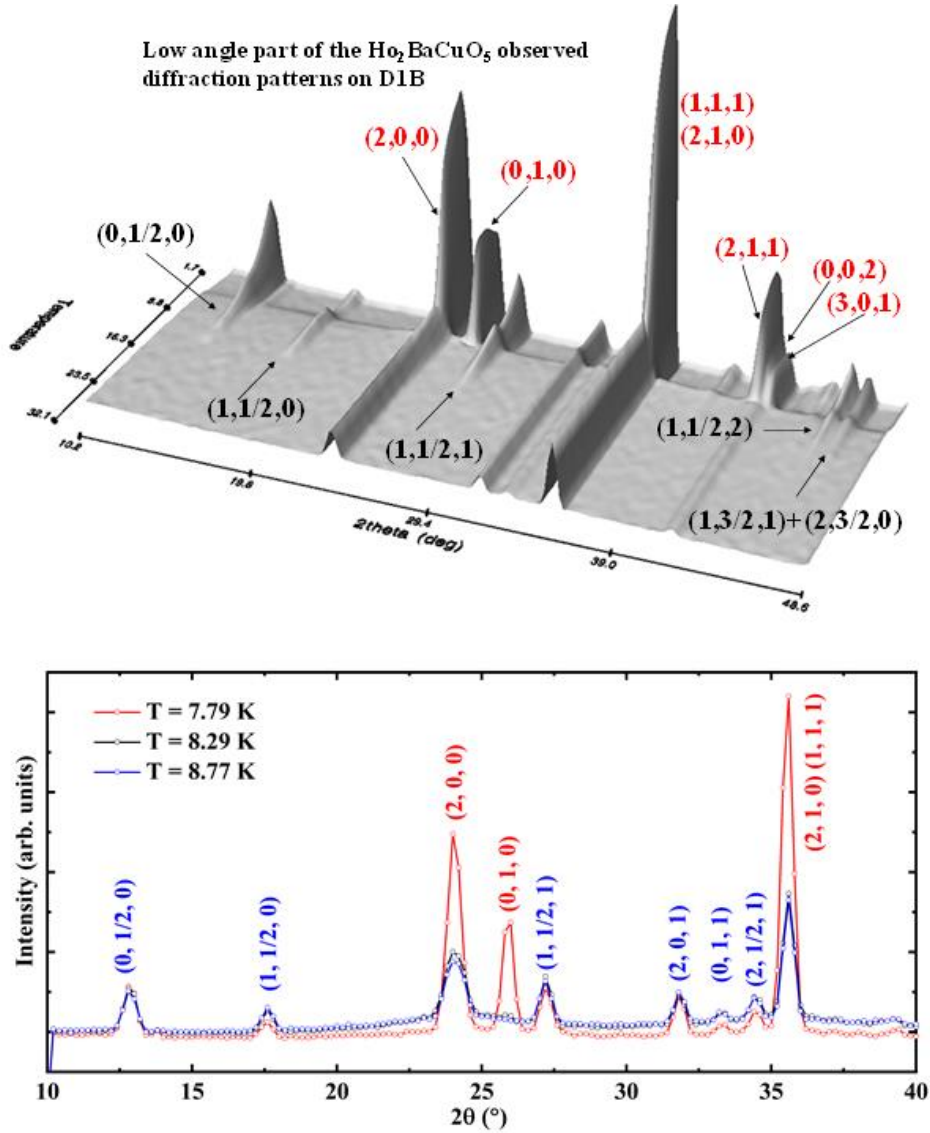


Figure S18. Refinement of the crystal and magnetic structure of $\text{Ho}_2\text{BaCuO}_5$ at $T = 8.3$ K (D1B, upper panel) and $T = 12$ K (WISH, bottom panel). Notice the different Q-range of both patterns. The bumps observed in D1B at $T = 8.3$ K is due to the short-range ordering of Ho moments corresponding to the $\mathbf{k} = (0, 0, 0)$ propagation vector that becomes long-range ordered just below 8 K. For the D1B data, we have used a single-phase described in the magnetic space group P_b112_1/n (standard setting P_a2_1/c) using symmetry modes and refining the amplitudes of the modes. The red tick marks are pure magnetic, the green marks are purely nuclear, and the blue ones are new nuclear reflections appearing in the new monoclinic group that is calculated as zero because we have maintained the constraints of $Pnma$ in the nuclear structure. In the case of WISH data, we have used three phases: the first one is the crystal structure described in the $Pnma$ group; the second phase corresponds to the magnetic described in P_b112_1/n without calculating the nuclear contribution and the third phase is an impurity of cubic Ho_2O_3 ($\approx 0.5\%$).

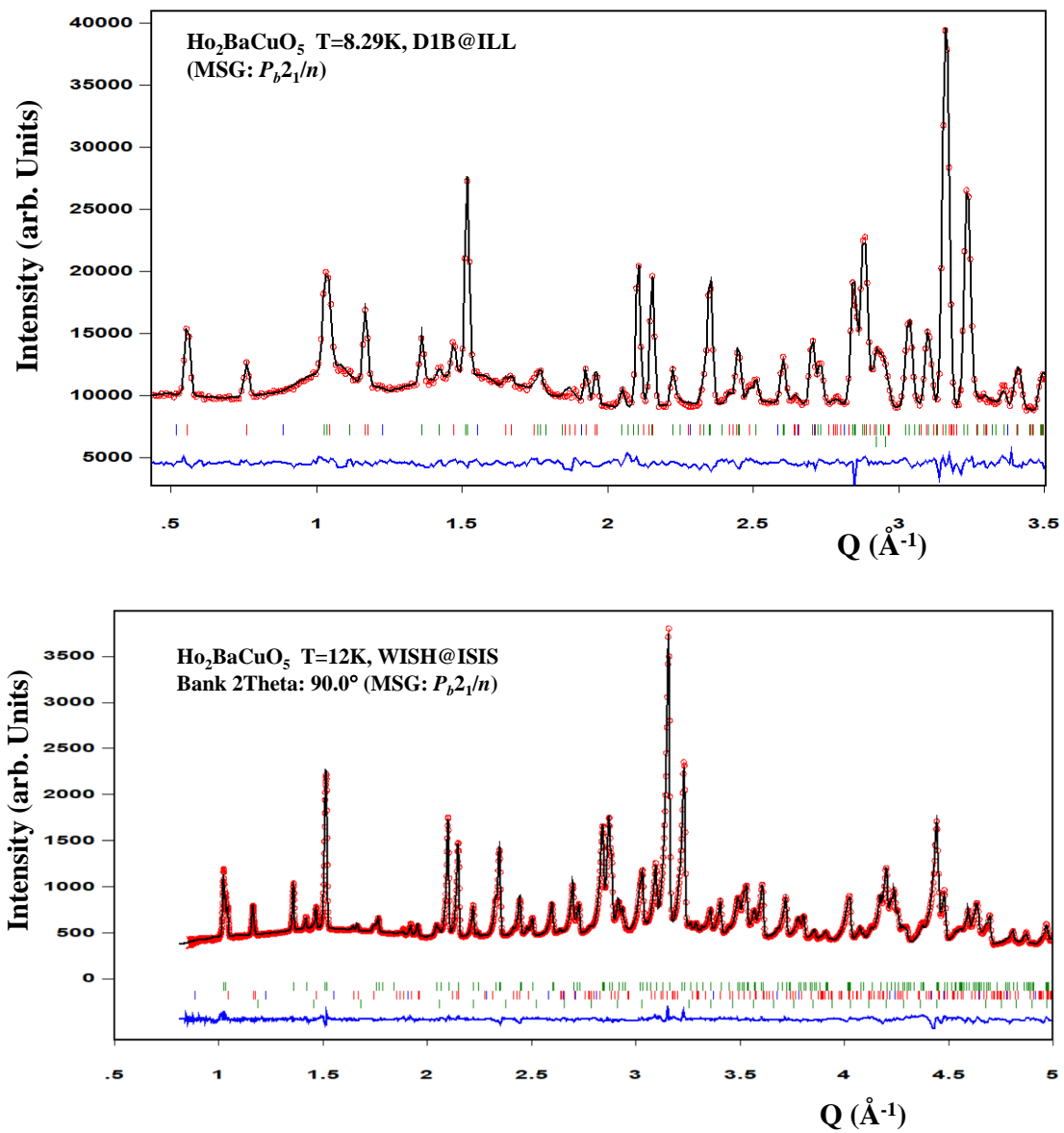


Figure S19. Representation of the magnetic structure of $\text{Ho}_2\text{BaCuO}_5$ at $T = 8.3$ K (D1B) in the magnetic space group P_b112_1/n . Only the magnetic atoms are represented, and the refinement was done by nullifying the components along \mathbf{b} for all atoms. The green atoms are Cu, the blue atoms correspond to the original Ho2 and the magenta atoms are Ho1, notice that Ho1 atoms bring a quite weak magnetic moment ≈ 0.42 (3) μ_B (8.3 K). The relative scale of magnetic moments is respected between the two temperatures except for the moments of Ho1 and Cu atoms that have been multiplied by 2 for display purposes.

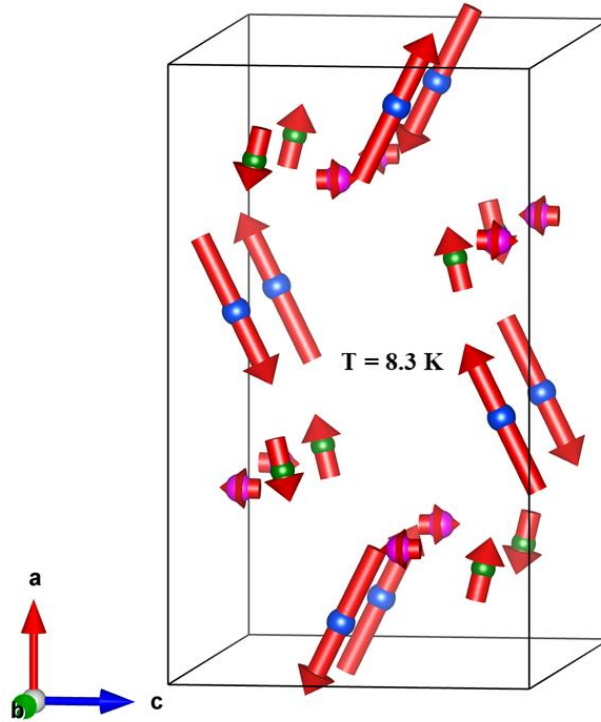
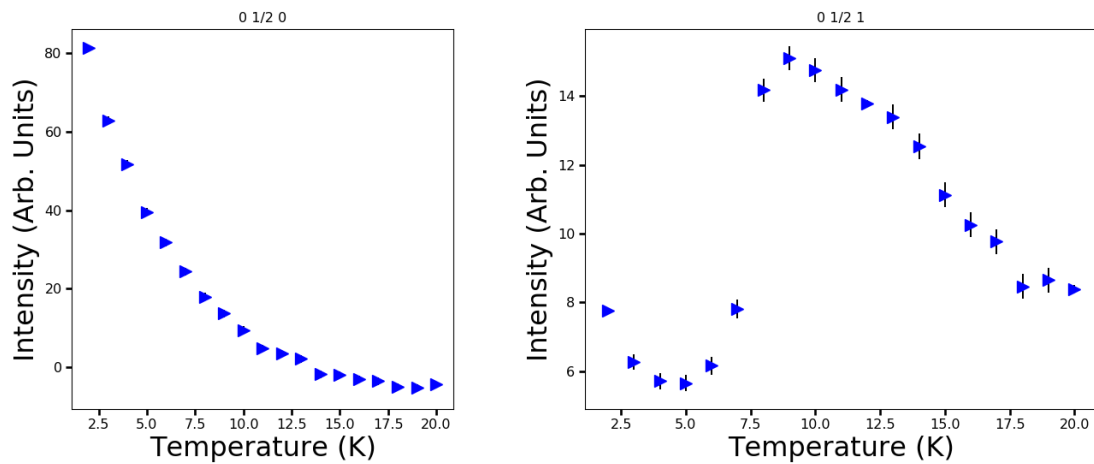


Figure S20. T -evolution of the Bragg reflections $(0 \frac{1}{2} 0)$ and $(0 \frac{1}{2} 1)$ of $\text{Ho}_2\text{BaCuO}_5$ obtained from WISH data.



Two magnetic phases refinement:

In general, the magnetic structure can be described as a Fourier series of the form:

$$\mathbf{m}_{jL} = \sum_{n=1}^{n=n_k} \mathbf{S}_{\mathbf{k}_n}^j e^{-2\pi i \mathbf{k}_n \mathbf{R}_L}$$

Where \mathbf{m}_{jL} is the magnetic moment of atom j in the unit cell with the origin at \mathbf{R}_L , n_k is the number of \mathbf{k} -vectors, and $\mathbf{S}_{\mathbf{k}_n}^j$ is the Fourier component of atom j for the \mathbf{k} -vector \mathbf{k}_n in the reference zero, $\mathbf{R}_L = (0,0,0)$, unit cell. In our case, the Fourier components are real vectors (magnetic moments) and the form adopted by the Fourier series is:

$$\mathbf{m}_{jL} = \mathbf{S}_{(0,0,0)}^j + \mathbf{S}_{(0,1/2,0)}^j e^{-\pi i L_y}$$

Where the L_y is integers obtained by the scalar product of the propagation vector \mathbf{k}_1 by the lattice vectors \mathbf{R}_L of the paramagnetic unit cell. The exponential factor is either 1 or -1, depending on if L_y is even or odd, respectively. The magnetic structure factor of a particular reflection indexed as $\mathbf{h} = \mathbf{H} + \mathbf{k}_n$ depends only on the Fourier coefficients $\mathbf{S}_{\mathbf{k}_n}^j$ so there is no interference between the reflections corresponding to different propagation vectors. A refinement of the structure considering independently the two propagation vectors and putting the symmetry constraints of the P_b112_1/n (\mathbf{k}_1) and $Pnm'a$ (\mathbf{k}_2) groups (essentially no component along the \mathbf{b} -axis for all atoms: $\mathbf{S}_{\mathbf{k}_n}^j = (m_{nx}^j, 0, m_{nz}^j)$, with $j = 1, 2, 3$ and $n = 1, 2$), gives an excellent fit to the experimental data for both TOF and CW data. See Fig. S21 (upper panel) for the D1B pattern at 2.3 K. The magnetic structure of $\text{Ho}_2\text{BaCuO}_5$ described in terms of the Fourier coefficients has then $3 \times (2 + 2) = 12$ free parameters. Notice that the group P_b112_1/n allows an additional component along \mathbf{b} , so strictly speaking there are $3 \times (2 + 3) = 15$ free parameters, but we have ignored this fact in the refinement presented in Fig. S21 (upper panel).

Figure S21. Refinement with two magnetic phases corresponding to two \mathbf{k} -vectors of D1B data at 2.3 K (upper panel) and $\chi^2 = 9.02$. The Fourier components verifying the symmetry of $Pnm'a$ $\{\mathbf{k} = (0, 0, 0)\}$ and P_b112_1/a $\{\mathbf{k} = (0, 1/2, 0)\}$. Refinement (with single magnetic phase) of D1B data at 2.3 K (bottom panel) using the magnetic space group $P112_1'/a$, $\chi^2 = 8.17$. The spikes near 70° and 86° corresponds to two, badly corrected by efficiency, detector cells. The two isolated tick marks around 73° correspond to two small peaks coming from the vanadium screens of the cryostat that are treated as a contribution to the background.

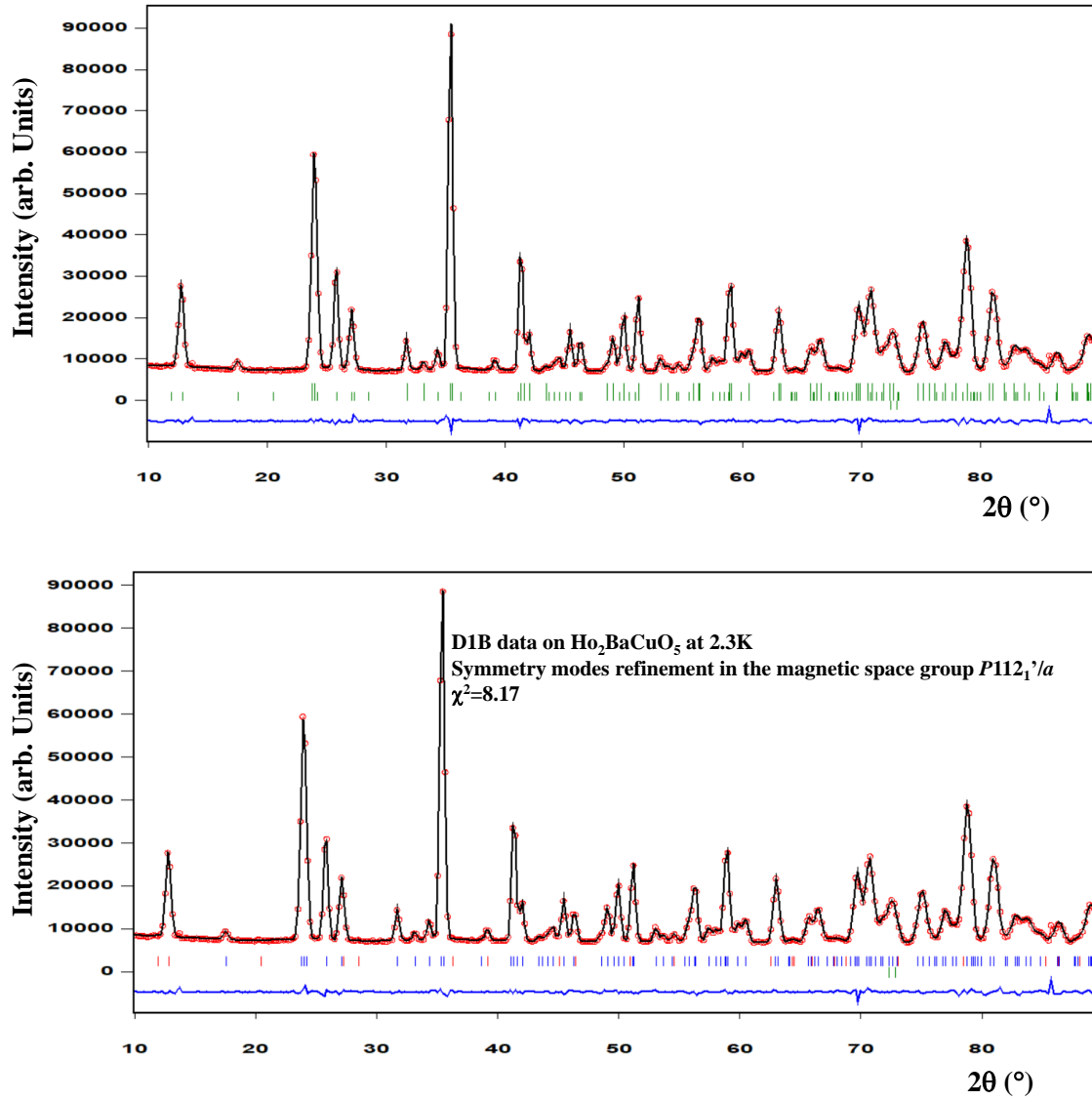


Table SIII. Crystal structure parameters of $\text{Ho}_2\text{BaCuO}_5$ at 12 K and 1.5 K, described in the Shubnikov groups P_6112_1/n and $P112_1'/a$ respectively and using symmetry modes. The constraints of the paramagnetic group, $Pnma1'$, have been applied by refining only displacive amplitudes (with respect to the paramagnetic structure at 20 K) corresponding to the identical representation GM_1^+ . The parameters correspond to the refinement of four banks of WISH data and the monoclinic angle has been fixed to 90° .

T = 12 K (P_6112_1/n)

	X	Y	Z	Biso
Ho1_1	0.28776 (11)	0.12500	0.1159 (2)	0.49 (3)
Ho2_1	0.07428 (13)	0.12500	0.39570 (20)	0.49 (3)
Cu_1	0.66042 (15)	0.12500	0.7115 (2)	1.07 (5)
Ba_1	0.9051 (2)	0.12500	0.9280 (3)	0.47 (6)
O1_1	0.43264 (14)	0.99660 (14)	0.16683 (15)	1.03 (4)
O1_2	0.93264 (14)	0.25340 (14)	0.33317 (15)	1.03 (4)
O2_1	0.22769 (11)	0.75297 (17)	0.3560 (2)	1.08 (5)
O2_2	0.72769 (11)	0.49703 (17)	0.1440 (2)	1.08 (5)
O3_1	0.10116 (20)	0.12500	0.0817 (3)	1.16 (5)

$a = 12.1663 (6)$, $b = 11.3106 (6)$, $c = 7.1137 (4)$ $\langle R\text{-Bragg} \rangle = 3.45\%$

T = 1.5 K ($P112_1'/a$)

	X	Y	Z	Biso
Ho1_1	0.28691 (20)	0.12500	0.1168 (3)	0.57 (6)
Ho1_2	0.28691 (20)	0.62500	0.1168 (3)	0.57 (6)
Ho2_1	0.07461 (11)	0.12500	0.3963 (2)	0.95 (6)
Ho2_2	0.07461 (11)	0.62500	0.3963 (2)	0.95 (6)
Cu_1	0.6599 (2)	0.12500	0.7105 (4)	1.16 (7)
Cu_2	0.6599 (2)	0.62500	0.7105 (4)	1.16 (7)
Ba_1	0.9062 (4)	0.12500	0.9274 (5)	0.64 (9)
Ba_2	0.9062 (4)	0.62500	0.9274 (5)	0.64 (9)
O1_1	0.4334 (2)	0.9958 (3)	0.1663 (2)	1.23 (6)
O1_2	0.4334 (2)	0.4958 (3)	0.1663 (2)	1.23 (6)
O1_3	0.9334 (2)	0.2542 (3)	0.3337 (2)	1.23 (6)
O1_4	0.9334 (2)	0.7542 (3)	0.3337 (2)	1.23 (6)
O2_1	0.22741 (19)	0.7528 (3)	0.3556 (4)	1.29 (7)
O2_2	0.22741 (19)	0.2528 (3)	0.3556 (4)	1.29 (7)
O2_3	0.72741 (19)	0.4972 (3)	0.1444 (4)	1.29 (7)
O2_4	0.72741 (19)	0.9972 (3)	0.1444 (4)	1.29 (7)
O3_1	0.1020 (3)	0.12500	0.0815 (5)	1.21 (9)
O3_2	0.1020 (3)	0.62500	0.0815 (5)	1.21 (9)

$a = 12.1613 (6)$, $b = 11.3081 (5)$, $c = 7.1130 (3)$ $\langle R\text{-Bragg} \rangle = 2.70\%$

Table SIV: Magnetic data extracted from the summary file of *FullProf* after refinement of four banks of WISH data at 12 K and D1B data at 8 K using magnetic symmetry modes.

=> Magnetic Moment Components and Standard Deviations at T = 12 K (WISH)

Atom	Mx	sMx	My	sMy	Mz	sMz	M	sM
Ho1_1	0.0201	0.0303	0.0000	0.0000	0.4924	0.0637	0.4928	0.0093
Ho2_1	1.8429	0.0669	0.0000	0.0000	1.3220	0.0612	2.2680	0.0102
Cu_1	-0.3354	0.0350	0.0000	0.0000	0.2839	0.0392	0.4395	0.0062

=> Amplitudes of magnetic symmetry modes in Bohr magnetons at T = 12 K (WISH)

	Amplitude	Sigma
A1_mY1	0.000000	0.000000
A2_mY1	0.020087	0.030303
A3_mY1	0.492324	0.063647
A4_mY1	0.000000	0.000000
A5_mY1	1.842855	0.066926
A6_mY1	1.321918	0.061218
A7_mY1	0.000000	0.000000
A8_mY1	-0.335422	0.034964
A9_mY1	0.283906	0.039153

<R-magnetic> = 7.56%

=> Magnetic Moment Components and Standard Deviations at T = 8.3 K (D1B)

Atom	Mx	sMx	My	sMy	Mz	sMz	M	sM
Ho1_1	-0.0109	0.0591	0.0000	0.0000	0.4241	0.2128	0.4242	0.0303
Ho2_1	2.8907	0.0626	0.0000	0.0000	1.4170	0.1611	3.2193	0.0232
Cu_1	-0.6237	0.0593	0.0000	0.0000	0.1496	0.1338	0.6414	0.0194

=> Amplitudes of magnetic symmetry modes in Bohr magnetons at T = 8.3 K (D1B)

	Amplitude	Sigma
A1_mY1	0.000000	0.000000
A2_mY1	-0.010916	0.059066
A3_mY1	0.423782	0.212654
A4_mY1	0.000000	0.000000
A5_mY1	2.888924	0.062531
A6_mY1	1.415972	0.160938
A7_mY1	0.000000	0.000000
A8_mY1	-0.623342	0.059284
A9_mY1	0.149515	0.133703

R-magnetic = 11.56%

Table SV: Magnetic data extracted from the summary file of *FullProf* after refinement of D1B data at 2.3 K. The values of magnetic moments obtained from the refinement at 1.5 K on WISH are also provided.

=> Magnetic Moment Components and Standard Deviations at T = 2.3 K (D1B)

Atom	Mx	sMx	My	sMy	Mz	sMz	M	sM
Ho1_1	7.1653	0.1213	0.0000	0.0000	0.8159	0.1409	7.2116	0.0222
Ho1_2	-2.5928	0.1213	0.0000	0.0000	2.8568	0.1409	3.8579	0.0222
Ho2_1	1.0515	0.1171	0.0000	0.0000	-8.4573	0.1680	8.5224	0.0255
Ho2_2	1.1704	0.1171	0.0000	0.0000	-8.3194	0.1680	8.4013	0.0255
Cu_1	-0.7717	0.1081	0.0000	0.0000	0.6528	0.1292	1.0107	0.0202
Cu_2	0.6867	0.1081	0.0000	0.0000	0.1673	0.1292	0.7068	0.0202

=> Amplitudes of magnetic symmetry modes in Bohr magnetons at T = 2.3 K (D1B)

	Amplitude	Sigma
A1_mY1	0.000000	0.000000
A2_mY1	4.874680	0.052245
A3_mY1	-1.019091	0.131627
A4_mY1	0.000000	0.000000
A5_mY1	-0.059403	0.060102
A6_mY1	-0.068837	0.143512
A7_mY1	0.000000	0.000000
A8_mY1	-0.728523	0.053872
A9_mY1	0.242409	0.120353
A10_mGM3-	0.000000	0.000000
A11_mGM3-	0.000000	0.000000
A12_mGM3-	0.000000	0.000000
A13_mGM4-	2.284233	0.109372
A14_mGM4-	1.833950	0.049805
A15_mGM4-	1.109978	0.100385
A16_mGM4-	-8.377424	0.086828
A17_mGM4-	-0.042449	0.093628
A18_mGM4-	0.409514	0.046660

R-magnetic = 1.73%

=> Magnetic Moment Components and Standard Deviations at 1.5 K (WISH)

Atom	Mx	sMx	My	sMy	Mz	sMz	M	sM
Ho1_1	7.4451	0.3499	0.0000	0.0000	0.9566	0.1454	7.5063	0.0353
Ho1_2	-2.6175	0.3499	0.0000	0.0000	3.0137	0.1454	3.9916	0.0353
Ho2_1	0.8831	0.0676	0.0000	0.0000	-8.5784	0.5150	8.6237	0.0726
Ho2_2	1.0110	0.0676	0.0000	0.0000	-8.7619	0.5150	8.8201	0.0726
Cu_1	-0.5614	0.0483	0.0000	0.0000	0.6087	0.0501	0.8281	0.0081
Cu_2	0.5150	0.0483	0.0000	0.0000	0.2527	0.0501	0.5736	0.0081

<R-magnetic> = 3.27%

Figure S22. Refinement of D1B data at 2.3 K using the magnetic space group $Pm'n2_1'$. The fit seems to be good but not as good as the fitting using two magnetic phases (see Fig. S21).

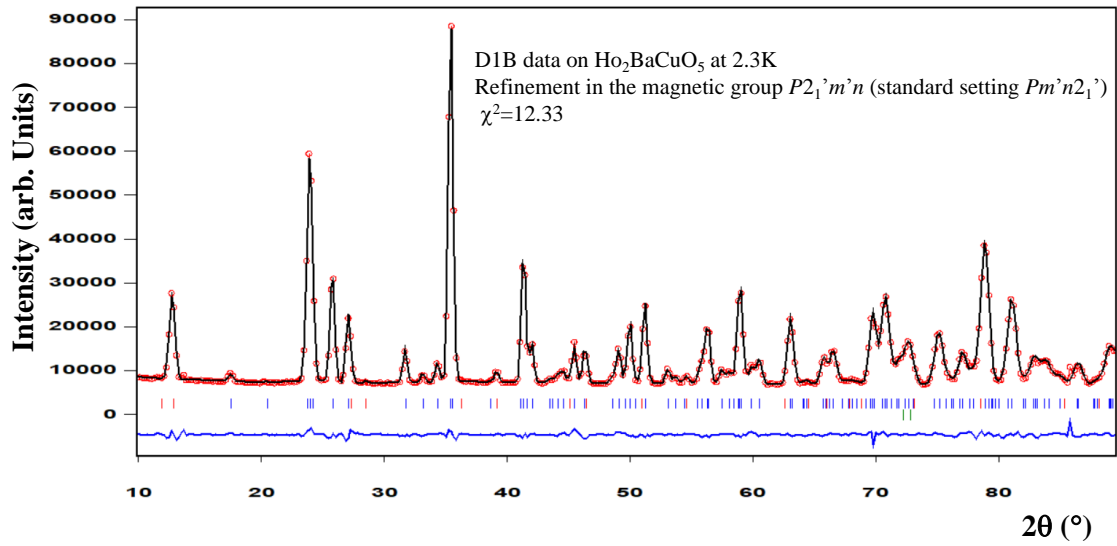


Figure S23-a. Evolution of magnetic symmetry mode amplitudes with temperature obtained from sequential refinements of D1B data. We have changed the sign of the refined amplitude $A_{16_mGM_3^-}$ to make the figure more readable. Notice that some amplitudes are interchanged at some high temperatures (A_{8_mY1} and A_{7_mY1}) reflecting instabilities of low values in the sequential refinements due to the fact that we have used the mode amplitudes of the three representations allowed by the magnetic space group.

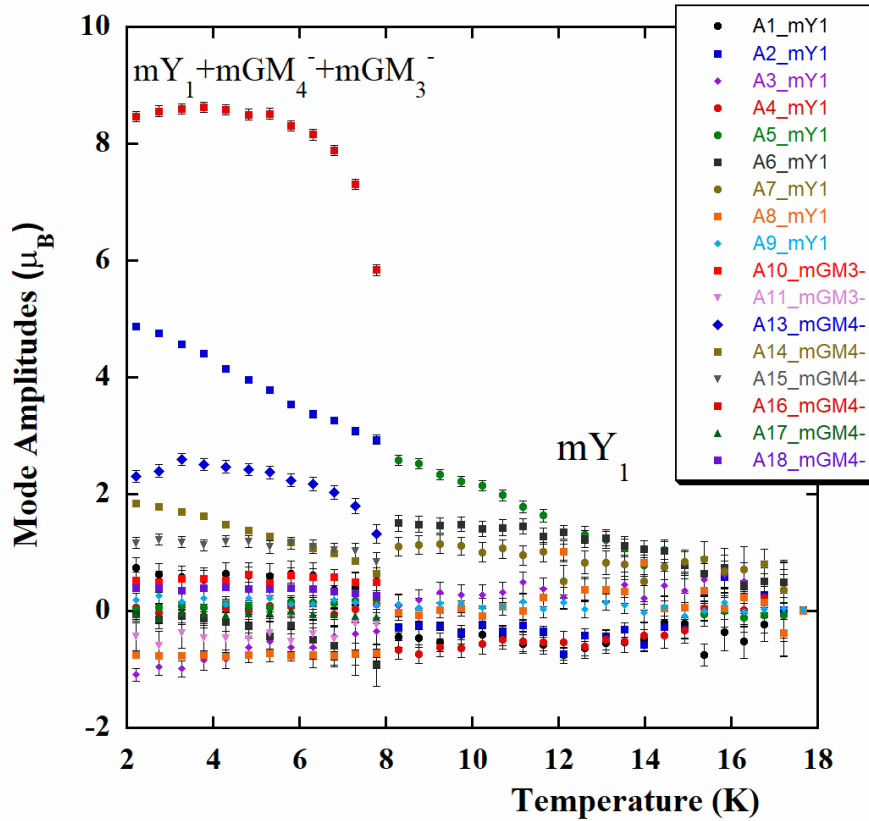


Figure S23-b. As S21-a but doing the refinements with no contribution of the mGM_3^- modes.

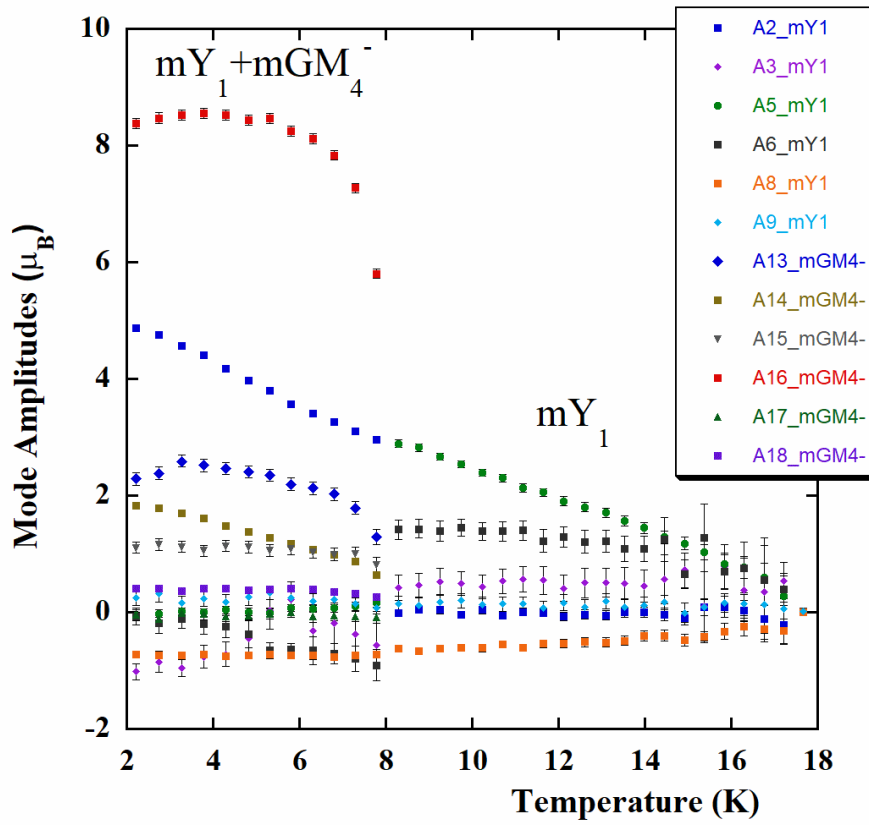


Figure S24. Magnetic moments of Ho_2BaCuO_5 as a function of temperature when the restriction of null components along \mathbf{b} is not applied.

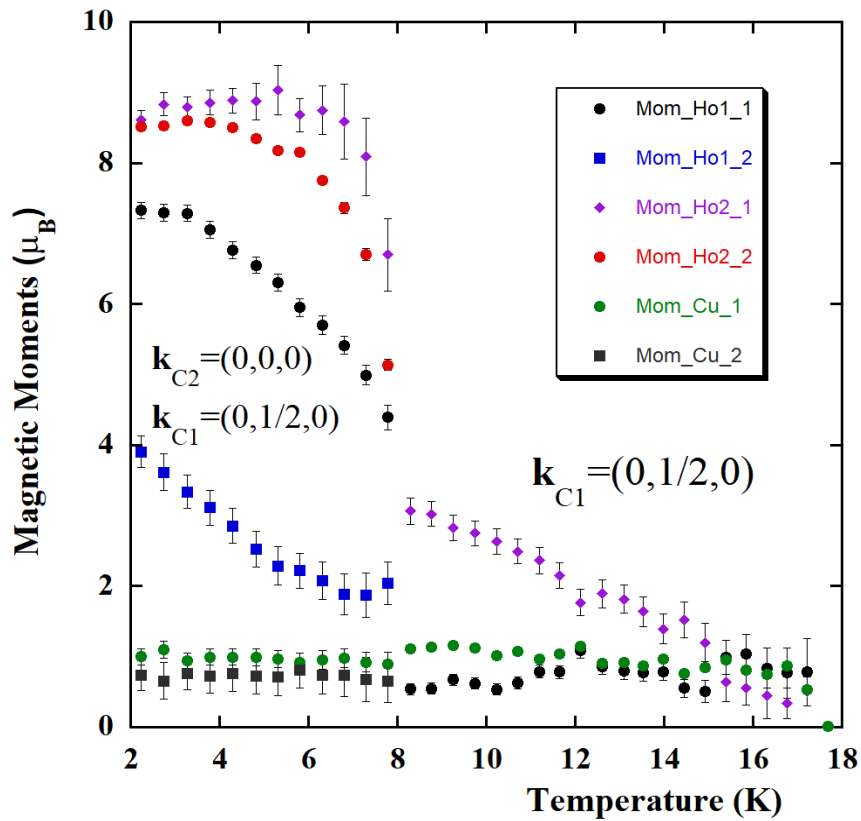


Figure S25. Magnetic moment components of Ho1 and Ho2 atoms of $\text{Ho}_2\text{BaCuO}_5$ as a function of temperature when the restriction of null components along \mathbf{b} is not applied.

